

# Effect of HRF spatial variability on the accuracy of multivariate Granger causal networks obtained from fMRI data

G. Deshpande<sup>1</sup>, and X. Hu<sup>1</sup>

<sup>1</sup>Department of Biomedical Engineering, Georgia Institute of Technology and Emory University, Atlanta, GA, United States

## Introduction

The hemodynamic response function (HRF) of fMRI data is known to vary across subjects and brain regions [1]. Since HRF variability may be dictated, in part, by non-neuronal considerations, it has the potential to confound inferences about directional neuronal influences obtained from Granger causality (GC) analysis of fMRI data [2]. However, a systematic investigation of this confound and its effect on the accuracy of Granger-based networks obtained from fMRI is lacking. Here, we investigate this aspect in a multivariate fashion using a simulated neuronal system.

## Methods

The ground truth for the causal interactions between neuronal systems was established using local field potentials (LFPs) obtained from the macaque cortex sampled at 1 KHz, owing to the very high temporal resolution they offer and the fact that they represent a direct measure of neuronal activity. In order to simulate multivariate causal relationships, we first sliced each LFP time series  $x(n)$  of length  $l$  into three parts,  $x_1(n)$ ,  $x_2(n)$  and  $x_3(n)$  with lengths  $l_1$ ,  $l_2$  and  $l_3$  ms, respectively, such that

$$\begin{aligned} x_1(n) &= x(n) \text{ for } n=l_3+d_2 \dots l \\ x_2(n) &= x(n) \text{ for } n=d_1 \dots d_1+l_2 \\ x_3(n) &= x(n) \text{ for } n=1 \dots l_3 \\ x_4(n) &= x(n) \text{ for } n=l_3 \dots d_1+l_2 \end{aligned}$$

According to this scheme,  $x_1(n)$  began  $d_2$  ms after the end of  $x_3(n)$  and  $x_2(n)$  began  $d_1$  ms after the beginning of  $x_3(n)$ . Consequently,  $x_1(n)$  leads  $x_2(n)$  by  $l_3 - d_1 + d_2$  ms and  $x_2(n)$  leads  $x_3(n)$  by  $d_1$  ms. Time series  $x_4(n)$  was defined to begin at  $l_3$  ms and end at  $l_3+d_1$  ms. Consequently,  $x_4(n)$  leads  $x_2(n)$  by  $l_3 - d_1$  ms and  $x_1(n)$  leads  $x_4(n)$  by  $d_2$  ms. Due to the above-mentioned delays between the time series, the network in Fig.1 is the ground truth from the neuronal data. This scheme was designed to incorporate a mediated influence from  $x_1(n)$  to  $x_3(n)$  via  $x_2(n)$  which should not be inferred as a direct connection from  $x_1(n)$  to  $x_3(n)$  in fMRI data since  $x_1(n)$  and  $x_3(n)$  do not have an overlap. Also, in addition to a direct connection from  $x_1(n)$  to  $x_2(n)$ , a mediated path via  $x_4(n)$  must be inferred since  $x_1(n)$  leads  $x_4(n)$ , which in turn leads  $x_2(n)$ . Since these types of situations are commonly observed in brain networks, we felt that it was important to model them in our multivariate simulations. However, when a region  $X$  drives region  $Y$ , the LFP pattern in  $Y$  may not be a time delayed replica of that in  $X$ . Therefore we assumed that the activity at  $Y$  is a weighted sum of its own intrinsic dynamics which is unrelated to  $X$  plus the delayed influence from  $X$ . Accordingly, we derived  $y_1(n)$ ,  $y_2(n)$ ,  $y_3(n)$  and  $y_4(n)$  from  $x_1(n)$ ,  $x_2(n)$ ,  $x_3(n)$  and  $x_4(n)$ , respectively, as shown in the equation below

$$y_j(n) = x_j(n) \quad \text{and} \quad y_j(n) = \left[ C \times x_j(n) \right] + \left[ (1 - C) \times y_j^{intrinsic}(n) \right] \quad \text{for } j = 2,3,4$$

In this formulation,  $x_1(n)$  was obtained from a single channel of LFP data and  $y_j^{intrinsic}(n)$  was obtained by randomizing the phase of a separate LFP channel for each  $j$  which was different from the one used to obtain  $x_1(n)$ . Thus, the intrinsic dynamics of  $y_j(n)$  not only had a magnitude spectrum different from that of  $x_j(n)$ , but also were also not causally related. Therefore, the causal relationship between  $y_1(n)$ ,  $y_2(n)$ ,  $y_3(n)$  and  $y_4(n)$  was determined by both the neuronal delays,  $d_1$  and  $d_2$ , and the factor  $C$ , which controlled the strength of the causal influence between them. We varied  $C$  from 0.5 to 1. When  $C=0.5$ , the contribution from the causal influence and intrinsic dynamics was equal and hence represents a weak causal influence because 50% of the phase in  $y_j(n)$  was drawn from a random process. On the other hand,  $C=1$  represents a strong causal influence as it is the case of a simple neuronal delay between the time series. The resulting simulated data were convolved with HRFs obtained from two gamma functions as in SPM2 [1], downsampled and measurement noise added to obtain simulated fMRI data with SNR=1 and TRs of 0.5,1,1.5 and 2 s, which were input into the Granger model in order to obtain fMRI-based GC networks. The rise times and time to peak for the HRFs assumed a random value between 0 and 2.5 s, which is the empirical upper limit of HRF variability across regions [1]. The neuronal delay was randomized between 0 and 500 ms. This simulation framework provided the capability to manipulate the causal relationship between the time series in addition to investigating the variability of HRF. The accuracy of the fMRI networks was obtained by comparing it with the ground truth obtained from the simulated LFP data (Fig.1) over 10,000 realizations of the system.

## Results and Discussion

Table.1 shows the percentage accuracy of the GC networks obtained from simulated fMRI data. It can be observed that higher causal influence (or lower intrinsic dynamics) and shorter TR resulted in higher accuracy. The accuracy of detecting each of the paths in the multivariate network individually, i.e. the accuracy of detecting a path in pair wise fashion, was higher compared to the accuracy of simultaneously detecting all of the paths correctly (multivariate case in Table.1). In experimental situations, researchers typically investigate multivariate brain networks and are constrained by the SNR provided by the scanner, the TR dictated by the requirement of whole brain coverage and the scanning time available, and the intrinsic dynamics, neuronal and hemodynamic delays inherent in the neurophysiological system under investigation. Therefore, the detection accuracies reported here are critical to determine the confidence that can be placed on multivariate GC networks derived from fMRI, given the SNR, TR and unknown neuronal and hemodynamic delays which are assumed to be in their normal physiological range. Implicit in the randomization of neuronal and hemodynamic delays is the assumption that they may not always oppose one another.

The performance of fMRI-based GC analysis in an actual experiment may be better or worse than predicted by us due to factors outlined below. First, the differences in HRF onset times and time to peak in experimental data may be driven by the underlying neuronal causality and may not always be hemodynamic in nature. Therefore, neuronal causality may explain part of the variance in HRFs across brain regions and hence the situation in experimental data may not be as dire as the one assumed in our simulations. Second, in experimental data, measurement noise is added only once during the acquisition while in our simulations, it was already present in the LFP data in addition to what we added to the simulated fMRI data. Consequently, the effective SNR of our simulations may be worse than what it seems. Third, pathological conditions may cause extreme discrepancies in HRFs of certain brain regions which may be more than 2.5 s [2]. While the former two factors may make the performance of GCA of fMRI perform better than our prediction, the third factor is likely to make it worse.

## Conclusions

We have investigated the performance accuracy of GC analysis of fMRI as a function of hemodynamic variability, neuronal delay, strength of causal influence and TR. Accordingly, faster sampling and stronger causal influences can lead to increased reliability of GC networks obtained from fMRI data.

## References

1. Handwerker et al. 2004. *NeuroImage* 21: 1639-51. 2. David et al. 2008. *PLoS Biology* 6(12): 2683-97.

**Acknowledgement:** NIH (R01 EB002009).

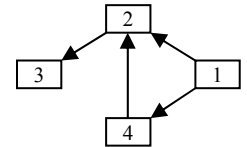


Figure 1 Ground truth of the multivariate network

Table 1 Percentage accuracy of the Granger-based fMRI network

TR	Multivariate				Pair wise			
	C=0.5	C=0.75	C=1	C=random[0.5,1]	C=0.5	C=0.75	C=1	C=random[0.5,1]
0.5	80	86	90	85	81	91	92	91
1.0	71	74	84	77	77	75	88	84
1.5	69	71	81	72	69	78	87	76
2.0	61	65	72	66	62	68	86	70